Computers, Materials & Continua

Tech Science Press

https://doi.org/10.32604/cmc.2026.084652

ARTICLE

Fusing Multi-Source Information for Reliability Assessment under Uncertainty: An Approach Integrating D-S Evidence Theory with Wiener Process Degradation Modeling

Ying Yan[1], **Yongqiang Yang**[2], **Cong Jiang**[3], **Bin Suo**[3] and **Kai Sun**[4,*]

[1]School of Economics and Management, Southwest University of Science and Technology, Mianyang, China
[2]Department of Statistics, School of Mathematics, Southwest Jiaotong University, Chengdu, China
[3]School of Information and Control Engineering, Southwest University of Science and Technology, Mianyang, China
[4]Institute of Microelectronics of the Chinese Academy of Sciences, Beijing, China

*Corresponding Author: Kai Sun. Email: sunkai1@ime.ac.cn

Received: 27 April 2026; Accepted: 04 June 2026; Published: 13 August 2026

ABSTRACT: Degradation data in practical reliability engineering are often scarce and heterogeneous, originating from multiple sources with varying degrees of uncertainty and conflict. Accordingly, this study proposes a hybrid framework that integrates Dempster–Shafer (D-S) evidence theory with the Wiener process for small-sample reliability assessment using multi-source heterogeneous data. First, a probabilistic non-uniform sampling method regularizes varied data sources and computes basic probability assignments (BPA). Second, a weight synthesis mechanism is constructed, where prior weights derived from prior knowledge are updated by evidence similarity quantified through the Expectation–Width (EW) distance, yielding posterior weights. Quantile sequences from each source are then fused via weighted aggregation to generate a time-series probability box. A Wiener process is subsequently employed to model the probability box (P-box) sequence, enabling interval reliability evaluation. Numerical simulations and a satellite gyroscope case study show that the method effectively fuses multi-source data, provides more comprehensive reliability intervals than single-source approaches, and significantly enhances evaluation robustness under small samples. The framework offers a systematic solution for multi-source data fusion and establishes a novel reliability assessment pathway under uncertainty, with broad applicability to aerospace and precision instrumentation systems.

KEYWORDS: Reliability assessment; multi-source data fusion; D-S evidence theory; Wiener process

1 Introduction

In the design, development, operation, and maintenance of modern high-end equipment and complex systems, such as aerospace vehicles and precision instruments, reliability, safety, and extended service life have become core design requirements [1]. These systems are typically characterized by high reliability, a long lifespan, and even zero-failure features, a condition that fundamentally challenges statistical evaluation methods predicated on traditional large-sample failure time data. Under the constraints of limited test durations and budgets, acquiring a sufficient quantity of field failure data is often infeasible [2]. Therefore, reliability assessment based on performance degradation data has become a mainstream approach to address the challenges of lifetime prediction for products characterized by small sample sizes and high reliability. By monitoring the degradation of critical performance parameters over time, degradation data rich with reliability information can be extracted even when the product has not experienced functional failure [3], thereby providing a novel and more practical data foundation for assessment.

Degradation paths in engineering systems frequently exhibit non-monotonic fluctuations driven by measurement noise, environmental variability, or inherent process randomness. The Wiener process naturally accommodates such behavior, and under a linear drift assumption, its first passage time follows an inverse Gaussian distribution with a closed-form reliability function [4]. This mathematical tractability, together with its clear physical interpretation, has made the Wiener process one of the most widely used stochastic models in degradation-based reliability analysis. To improve modeling realism, many recent studies have extended the classical Wiener-process framework in different directions. A central challenge in degradation modeling is capturing unit-to-unit variability among nominally identical products. To address this, Wu et al. [5] proposed a nonlinear Wiener process model in which the drift coefficient follows a closed skew-normal distribution, allowing asymmetric variability in degradation behavior to be represented. Along a similar line, Hu et al. [6] incorporated damage resistance and external shock effects into a nonlinear Wiener process framework for reliability analysis. Beyond individual differences, many degradation processes also evolve through multiple stages or phases. In the small-sample regime where maximum likelihood estimators tend to be unreliable, Wang et al. [7] investigated belief reliability modeling for two-phase degradation systems with a change point. Extending this line of work to practical engineering components, Zeng et al. [8] applied a two-phase nonlinear Wiener process to the sealing degradation analysis of deep-water pipeline connectors, while Ma et al. [9] developed a multi-phase Wiener process degradation model that accounts for imperfect maintenance activities. Measurement uncertainty introduces another important challenge in degradation analysis. To handle this issue, Guan et al. [10] proposed a two-stage Wiener-process-based degradation modeling approach that considers measurement errors in remaining useful life prediction. For systems whose reliability depends on multiple correlated degradation modes, Zheng et al. [11] combined Wiener processes with random effects and D-vine copulas for complex-system reliability estimation. More recently, Wiener-process-based degradation modeling has been integrated with data-driven methods. Collectively, these studies have extended Wiener-process-based reliability modeling to more complex and realistic engineering settings.

Although these extensions have substantially improved the flexibility and applicability of Wiener-process-based degradation models, their effectiveness still depends heavily on the availability of sufficient degradation data for parameter estimation and model validation. In practical engineering applications, such data are often scarce, heterogeneous, and subject to various sources of uncertainty. The information available for reliability assessment can originate from accelerated life tests conducted under different stress levels, historical data from similar products, real-time field monitoring, numerical simulations, and expert knowledge. Effectively integrating such multi-source information for reliability assessment under small-sample conditions has therefore become an important research issue. Current mainstream approaches to this problem include Bayesian methods, Dempster–Shafer (D-S) evidence theory, and machine-learning-based methods, each offering distinct advantages in handling uncertainty, combining heterogeneous evidence, and extracting patterns from complex data, respectively [12]. Although Bayesian methods have demonstrated unique advantages in fusing multi-source prior information with small-sample field data [13,14], and have achieved fruitful results in comprehensive assessments based on lifetime data, they still lack a systematic fusion and modeling framework when dealing with multi-source, heterogeneous degradation data. The D-S evidence theory has garnered considerable attention because it does not require prior probabilities and can effectively handle uncertainty [15,16]. This theory uses basic probability assignments (BPAs) to represent evidence for both single and multiple subsets, enabling it to effectively characterize the uncertainty inherent in information and providing a powerful tool for tasks such as data fusion [17,18]. Considerable progress has been made in degradation modeling and multi-source data fusion. However, most existing studies focus on single data sources or idealized identically distributed data, failing to systematically address the three key issues arising from data multi-source heterogeneity, which constitutes a limitation of the current literature.

First, regarding multi-source information fusion techniques, the advantage of D-S evidence theory lies in its ability to operate without prior probabilities and its capacity to effectively represent data uncertainty. However, in the field of reliability assessment, particularly for continuously degrading performance parameters, research on extending D-S evidence theory from traditional applications such as fault diagnosis and multi-sensor fusion to the fusion and uncertainty quantification of continuous degradation trajectory data itself remains scarce. Existing applications are largely confined to qualitative or discrete state judgments and have not been deeply integrated with continuous-time stochastic process models.

Second, in the statistical modeling of degradation data, single-source degradation modeling based on Wiener processes, Gamma processes, and the like has become quite mature. Researchers have developed random effects models that account for individual differences, and lifetime extrapolation methods based on acceleration models. However, when confronted with degradation data from multiple sources, with uneven sample sizes and even varying distributional characteristics, a fundamental question emerges: how to establish a unified and comparable "dialogue" platform for these heterogeneous data? Most studies either choose to ignore part of the data or simply perform data splicing, lacking a preprocessing and feature extraction method that can objectively measure the credibility of different data sources and perform weighted fusion accordingly. This leads to the uncertainty inherent in the model input being improperly handled, which in turn affects the robustness of the final assessment results.

Finally, at the level of comprehensive reliability assessment frameworks, although some studies have attempted to use Bayesian theory to fuse accelerated test data with field data, these frameworks often rely on assumptions that the data follow specific distributions (such as the Weibull distribution), which limits their applicability to more general degradation data scenarios. More importantly, existing frameworks commonly suffer from a disconnection problem: the data fusion module and the subsequent stochastic process modeling module are often separate, failing to form a seamless closed loop that proceeds from multi-source heterogeneous data input, to uncertainty fusion and representation, and then to continuous-time degradation modeling and interval reliability assessment. This disconnection results in significant information loss during the evaluation process, and the uncertainty in the final outcomes can hardly be traced back to the original differences among data sources.

In summary, the gaps in existing research can be summarized as follows:

- A lack of a systematic methodology for applying D-S evidence theory to feature extraction, conflict evidence reconciliation, and uncertainty fusion for multi-source continuous degradation data;
- The absence of an objective, data-driven mechanism for determining the weights of multi-source heterogeneous degradation data in the fusion process;
- The lack of a comprehensive framework that seamlessly connects the results of multi-source data fusion (e.g., probability distributions, probability boxes) with stochastic degradation models such as Wiener processes, thereby enabling the complete propagation of uncertainty from the data level to the assessment outcome level.

To address the above issues, this paper aims to establish a unified framework for multi-source degradation data analysis and comprehensive reliability assessment. The core idea is to connect heterogeneous data preprocessing, uncertainty fusion, and stochastic degradation modeling into a coherent analytical process, so that the uncertainty introduced by differences among data sources can be consistently represented and propagated throughout the reliability assessment procedure. Specifically, this study focuses on three key aspects: the construction of a comparable feature representation for heterogeneous degradation data, the objective fusion of conflicting multi-source information, and the integration of fusion results with Wiener-process-based degradation modeling. Through this framework, the proposed method seeks to provide a more complete and robust reliability assessment approach for multi-source degradation scenarios.

First, we propose a full-process analysis framework encompassing data preprocessing, uncertainty characterization, feature fusion, and statistical modeling. Focusing on the core aspect of multi-source data fusion at specific time points, this study develops the following key methods: a feature extraction method based on probabilistic non-uniform sampling is proposed to regularize samples of different sizes, thereby addressing the data "dialogue platform" problem; a two-stage weight synthesis mechanism is constructed, integrating prior knowledge (data source reliability) with inter-evidence similarity (based on an improved EW Distance) to determine fusion weights objectively and adaptively, responding to the challenge of weight determination; subsequently, the Dempster-Shafer (D-S) evidence theory framework is employed for weighted fusion, generating a probability box representation at each time point; and an area metric is introduced to quantitatively evaluate the fusion effect, achieving explicit uncertainty representation.

Second, this paper deeply integrates the time-series probability box data obtained from fusion with the Wiener stochastic process, thereby bridging the disconnection in the analytical chain. By modeling the fused interval-valued degradation trajectories, an interval reliability assessment method is proposed, which completely characterizes the full-chain uncertainty propagation process from data input and fusion processing to modeling and evaluation.

The theoretical contribution of this study lies in being the first to systematically apply D-S evidence theory to weight synthesis and fusion for multi-source continuous degradation data, forming a logical closed loop with Wiener process modeling, and providing a new "data-evidence-model" methodological paradigm for reliability assessment under uncertainty. The practical contribution is that the proposed framework offers a directly applicable solution for accurate reliability assessment of complex equipment under conditions of multi-source, heterogeneous, and small-sample data. Validation through engineering cases, such as satellite gyro components, demonstrates that compared to methods relying on a single data source or simple fusion, this method can provide more reasonable and complete reliability assessment intervals, significantly improving the robustness and engineering credibility of the evaluation results.

The remainder of this paper is organized as follows. Section 2 outlines the overall analytical framework for multi-source degradation data. Section 3 elaborates on the multi-source data fusion method at specific time points, including uncertainty characterization, feature extraction, weight determination, and fusion algorithms. Section 4 introduces product degradation modeling based on the Wiener process, along with interval reliability assessment and performance evaluation. Section 5 validates the effectiveness of the proposed method through numerical simulations and engineering case studies. Finally, conclusions are drawn.

2 Analytical Framework for Multi-Source Degradation Data

In engineering practice, when performing fusion assessment on product degradation data from multiple sources such as numerical simulation, semi-simulation testing, and actual product testing, the following characteristics are often observed:

- Sample sizes vary considerably across sources. numerical simulation and laboratory accelerated test data are often abundant, whereas actual product testing and field data are generally scarce.

- The credibility of different data sources differs systematically. Actual product testing and field data possess high credibility, while digital simulation and laboratory accelerated test data are comparatively less reliable.
- Population heterogeneity. Inherent discrepancies exist between simulation models (whether numerical or semi-simulation) and the actual physical equipment they represent; similarly, data collected from similar products of different model variants are not identically distributed. Consequently, these multiple data sources manifest as heterogeneous populations requiring specialized fusion treatment.

Given the significant differences in representation forms, uncertainty, and credibility among product degradation datasets, it is necessary to effectively handle uncertainty, accommodate conflicting information, and achieve data fusion without relying on prior distributions. The fused data represent the performance degradation of products at different time slices, and the degradation increments exhibit randomness, which conforms to a continuous-time stochastic process. Therefore, the Wiener process—which can effectively account for uncertainty and more comprehensively reflect the range of possible outcomes—is selected to model the degradation data, thereby characterizing the product's degradation process.

Consider multiple independent monitoring data streams acquired from the same product unit, which reflect the product's degradation state from different perspectives. Due to differences in sensor characteristics, monitoring principles, and sampling conditions, these data streams are inherently asynchronous and heterogeneous discrete-time sequences. Their mathematical description is as follows:

Let the total observation period be T. There are M data sources, each of which takes independent samples during this period, forming the original observation sequences. For the i-th data source $X^i(t)$, obtains an observation $x^i\left(t_1^i\right), x^i\left(t_2^i\right), \cdots x^i\left(t_{N_i}^i\right)$ at time points $t_1^i, t_2^i, \cdots t_{N_i}^i$, the number of sampling points is N_i and $t_k^i \in [0, T]$. Typically, the number of sampling points varies across different data sources, exhibiting asynchronicity. Additionally, the degradation measures from different sources may have distinct dimensions, precision levels, and reliability characteristics, exhibiting heterogeneity. These data collectively constitute noisy and uncertain partial observations of the underlying, true but not directly observable degradation process $X(t)$ of the product. By leveraging the aforementioned multi-source information to address the problem of incomplete or unreliable information from a single data source, outputs at two levels are ultimately generated:

- A unified fused degradation time-series sequence: a degradation state sequence defined on a continuous or dense time scale that comprehensively considers information from different data sources. This sequence should be smoother, more robust, and closer to the true degradation trend than any sequence from a single data source.
- A parameterized degradation process model: a stochastic degradation process model estimated based on the sequence, where represents the set of model parameters. This model can quantitatively describe the mean degradation trajectory and its associated uncertainty.

To achieve the transformation from the aforementioned inputs to the outputs, this paper proposes a systematic framework comprising four core tiers, as shown in Fig. 1.

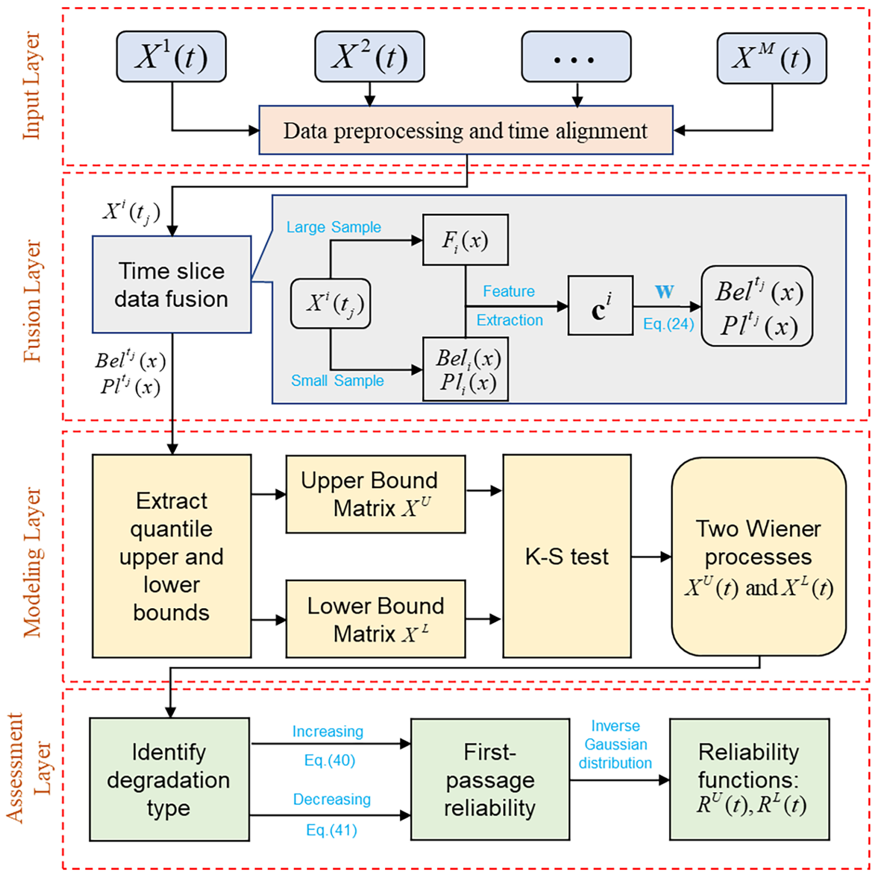

Figure 1: Analytical framework for reliability assessment using multi-source degradation data.

3 Time-Slice Based Degradation Data Fusion

To address the heterogeneity issues in multi-source degradation data (including differences in sample size, forms of uncertainty representation, and data source credibility), this paper proposes a weighted quantile-based fusion method. This section focuses on the uncertainty representation and fusion of heterogeneous degradation data at each observation time point, aiming to transform multi-source degradation observations into unified P-Box representations for subsequent stochastic degradation modeling. As shown in Fig. 2, the proposed method mainly consists of the following four steps:

1. Uncertainty representation of degradation data: For large-sample data (such as numerical simulation data and semi-simulation testing data), probability distributions can be used for characterization; for small-sample data (such as actual product testing data), the Probability Box (P-Box) is employed. The P-Box is a mathematical tool for representing uncertainty that provides upper and lower probability bounds, which can effectively capture uncertainty in the data.
2. A feature extraction method based on probabilistic non-uniform sampling is proposed, which extracts corresponding points from the probability distribution of large-sample data based on the upper and lower bounds of the P-Box obtained from small-sample data in the previous step, thereby facilitating subsequent weight calculation.
3. Determination of multi-source data weights: The credibility of multi-source data is expressed through weights, which consist of two components: prior weights and posterior weights. Prior weights are determined by the data source characteristics. For instance, outputs from simulation models are generally

assigned lower weights, while actual product testing data receive higher prior weights due to their greater acceptance. Posterior weights are determined by the empirical performance of the data, considering factors such as sample size differences, sample uncertainty, and inter-sample similarity, thereby enabling objective weighting. By synthesizing these two types of weights, comprehensive subjective-objective weights are obtained.

4. An evidence fusion method based on comprehensive weights to achieve multi-source data fusion.

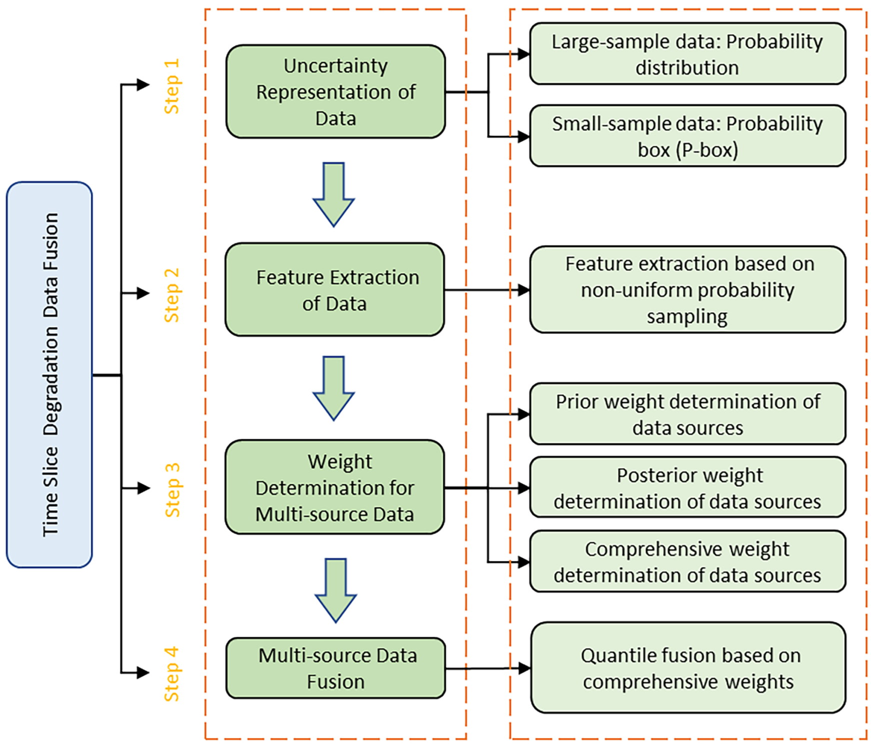

Figure 2: Multi-source data fusion framework.

3.1 Uncertainty Characterization of Data

To enable subsequent fusion of heterogeneous degradation data from different sources, the uncertainty information contained in the original observations is first transformed into a unified representation form. Suppose that at time t_j, there are two sets of data, $X^S = \left\{x_1^S, x_2^S, \cdots, x_{nS}^S\right\}$ and $X^L = \left\{x_1^L, x_2^L, \cdots, x_{n_L}^L\right\}$, where $n_S < n_L$, X^S is small-sample data and X^L is large-sample data.

Since the sample size of X^L is large, its probability distribution $F_L(x)$ can be obtained through maximum likelihood estimation (MLE). For example, when the sample follows a normal distribution, the MLE of its distribution parameters can be calculated as follows:

$$\begin{cases} \hat{\mu} = \frac{1}{n}\sum\limits_{i=1}^{n} x_i \\ \hat{\sigma}^2 = \frac{1}{n-1}\sum\limits_{i=1}^{n} \left(x_i - \hat{\mu}\right)^2 \end{cases} \tag{1}$$

where n denotes the sample size.

For small-sample data X^S, distribution parameters obtained directly through MLE often exhibit considerable uncertainty. To address this issue, this paper introduces the Probability Box (P-Box) method based on D-S evidence theory for characterization. First, the original sequence X^S is arranged in ascending order to obtain an ordered sequence $x_{(1)}, x_{(2)}, \cdots, x_{(n)}$, and let:

$$\begin{cases} y_{(1)} = x_{(1)} \\ y_{(n+1)} = x_{(n)} \\ y_{(i)} = \left(x_{(i-1)} + x_{(i)}\right)/2. \quad i = 2, 3, \cdots, n \end{cases} \tag{2}$$

The sequence $y_{(i)}$ partitions the interval $\left[x_{(1)}, x_{(n)}\right]$ into n mutually disjoint subintervals. These n subintervals are taken as the focal elements of this data source:

$$c_i = \left(y_{(i)}, y_{(i+1)}\right] \tag{3}$$

For each focal element C_i defined above, the deviation degree is introduced to characterize the dispersion of the interval relative to the overall sample center. Considering that each focal element is represented by an interval with lower and upper bounds, a two-dimensional Euclidean distance based on both endpoints is adopted to jointly measure the positional deviation of the interval. Compared with simpler measures such as interval width alone, this geometric measure simultaneously incorporates both the spread and location information of the interval, thereby providing a more comprehensive characterization of uncertainty. The deviation degree s_i is defined as follows:

$$\begin{cases} s_i = \frac{l_i}{\sum_{j=1}^{n} l_j} \\ l_i = \sqrt{\frac{(y_i - \overline{x})^2 + (y_{i+1} - \overline{x})^2}{2}} \end{cases} \tag{4}$$

Here, the sample mean is used as the reference center to reflect the overall central tendency of the degradation observations. Then, the basic probability assignment (BPA) for each focal element is defined through the deviation degree:

$$m\left(c_i\right) = \frac{1 - s_i}{\sum_{j=1}^{n} 1 - s_j} \tag{5}$$

Subsequently, two fundamental functions characterizing uncertainty within the evidence theory framework are derived: the belief function $Bel_S\left(x\right)$ and the plausibility function $Pl_S\left(x\right)$:

$$\begin{cases} Bel_S\left(x\right) = \sum\limits_{c_i \subseteq (x_1, x)} m\left(c_i\right) = \sum\limits_{j=1}^{j_x - 1} m\left(c_j\right), \left(x \in c_{j_x}\right) \\ Pl_S\left(x\right) = \sum\limits_{c_i \cap (x_1, x)} m\left(c_i\right) = \sum\limits_{j=1}^{j_x} m\left(c_j\right). \left(x \in c_{j_x}\right) \end{cases} \tag{6}$$

The belief function can be viewed as the lower bound of the probability that event A is true, while the plausibility function can be viewed as the upper bound of the probability that event A is true [19].

3.2 Feature Extraction Method Based on Non-Uniform Probability Sampling

Building upon the uncertainty representations obtained in the previous section, this part focuses on extracting comparable features from both small-sample and large-sample degradation data to enable unified uncertainty representation. To achieve effective fusion of small-sample P-Box representations and large-sample continuous distributions within a consistent framework, a feature extraction method based on non-uniform probability sampling is proposed. The core idea is to map different data representations into comparable quantile sequences under identical probability levels, thereby providing a unified basis for subsequent uncertainty fusion.

As shown in Fig. 3, by performing non-uniform probability sampling on the probability distribution $F_L(x)$ of X^L at probability levels $q_i = \sum_{j=1}^{i-1} m(c_j), (i = 2, 3 \cdots n)$, along the probability axis (vertical axis), a set of quantile sequences $y'_{(1)}, y'_{(2)}, \cdots, y'_{(n)}$ is obtained. Taking $y'_{(1)} = \min\{X^L\}$, $y'_{(n+1)} = \max\{X^L\}$, the focal elements of the sequence X^L are then obtained as:

$$c'_i = \left(y'_{(i)}, y'_{(i+1)}\right]. (i \in \{1, 2, \cdots, n\}) \tag{7}$$

According to the properties of this sampling method, it can be seen that:

$$m(c'_i) = m(c_i) \tag{8}$$

After non-uniform probability sampling, the data characteristics of sequences X^S and X^L are uniformly represented in the form of focal elements and BPAs. Both sequences share the same BPA, with the difference lying in their focal elements. Therefore, in subsequent data fusion, the similarity between X^S and X^L can be measured by evaluating the similarity between their respective focal elements.

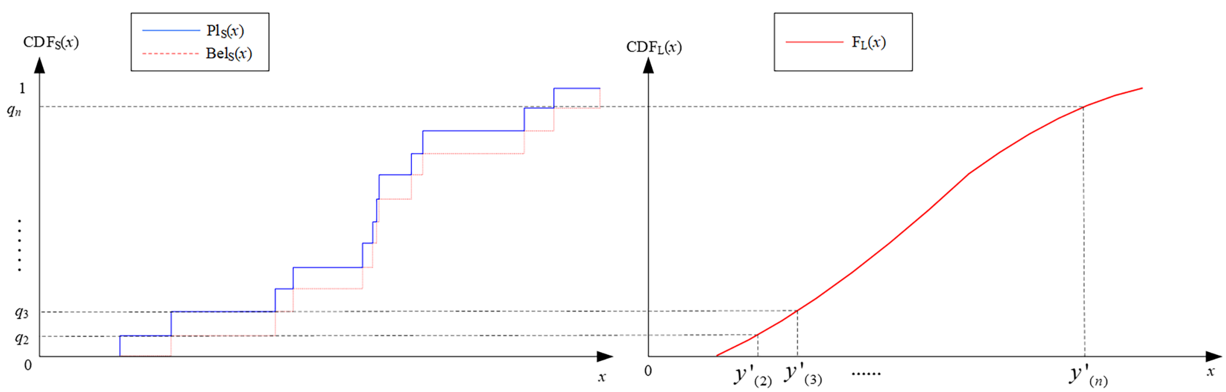

Figure 3: Feature extraction method based on non-uniform probability sampling.

3.3 Weight Determination Method for Multi-Source Data

The fusion weights of multi-source degradation data are determined based on the evidence bodies obtained in the previous section. In this study, the relative reliability of each evidence source is quantitatively characterized to provide an objective basis for subsequent fusion. Suppose there are M data sources and after unified representation, each data source has n focal elements. The multi-source data are processed using the feature extraction method based on non-uniform probability sampling to obtain multi-source evidence bodies. The focal elements of the k-th evidence source and the l-th evidence source can be expressed as:

$$\begin{cases} \mathbf{c}^k = \left[c_1^k, c_2^k, \cdots, c_n^k\right], c_i^k = \left[y_{(i)}^k, y_{(i+1)}^k\right] \\ \mathbf{c}^l = \left[c_1^l, c_2^l, \cdots, c_n^l\right]. \ c_i^l = \left[y_{(i)}^l, y_{(i+1)}^l\right] \end{cases} \tag{9}$$

And the BPAs are:

$$m\left(c_i^k\right) = m\left(c_i^l\right). \ i \in \{1, 2, \cdots, n\} \tag{10}$$

The two evidence sources have different focal elements but the same BPA. Since both focal elements c_i^k and c_i^l are interval numbers, a similarity measure between the evidence sources can be obtained based on the distance between these intervals.

To meet the requirements of practical problems, various distance measures for interval numbers have been proposed, such as the P-distance [19] and the Hausdorff distance [20]. The P-distance introduces a parameter p to adjust the sensitivity of the distance measure and is computationally tractable. The Hausdorff distance captures the worst-case deviation between sets. However, these distance measures are typically defined based only on the endpoints of intervals, which may lead to loss of useful information. Therefore, this paper adopts an Expectation–Width (EW) distance measure, which incorporates both central tendency and dispersion information of intervals while maintaining computational simplicity. The definition of the interval distance is given below.

Definition 1: *Let R be the real number field, $\overline{x}, \underline{x} \in \mathbf{R}$, and $\underline{x} \le \overline{x}$. If $I = (\underline{x}, \overline{x})$, then I is called an interval number; $E(I) = (\overline{x} + \underline{x})/2$ is the expected value of I; $B(I) = (\overline{x} - \underline{x})/2$ is the width of I [21].*

Definition 2: *Let $I_1 = (\underline{x}_1, \overline{x}_1)$ and $I_2 = (\underline{x}_2, \overline{x}_2)$ be two interval numbers. Then their distance is defined as [21]:*

$$d(I_1, I_2) = \sqrt[q]{|E(I_1) - E(I_2)|^q + \frac{1}{3}|B(I_1) - B(I_2)|^q} \tag{11}$$

where $q \ge 1$, and $q = 2$ is typically taken. When $q = 2$, the EW distance between two focal elements c_i^k and c_i^l can be obtained as:

$$d_i^{k,l} = \sqrt{\left|E\left(c_i^k\right) - E\left(c_i^l\right)\right|^2 + \frac{1}{3}\left|B\left(c_i^k\right) - B\left(c_i^l\right)\right|^2} \tag{12}$$

Furthermore, the EW distances between all corresponding pairs of focal elements from the k-th and l-th evidence sources can be obtained as:

$$\mathbf{d}^{k,l} = \begin{bmatrix} d_1^{k,l} & d_2^{k,l} & \cdots & d_n^{k,l} \end{bmatrix} \tag{13}$$

Given that the basic probability assignment corresponding to the i-th focal element is p_i, the comprehensive distance measure between the k-th and l-th evidence sources is:

$$D^{k,l} = \left[d_1^{k,l}, d_2^{k,l}, \cdots d_n^{k,l}\right] \cdot \left[p_1, p_2 \cdots p_n\right]^T \tag{14}$$

Normalize it:

$$\hat{D}^{k,l} = D^{k,l} / \max_k \left\{ \max_l \left\{ D^{k,l} \right\} \right\}. \tag{15}$$

Define the similarity between two evidence sources as:

$$S^{k,l} = 1 - \hat{D}^{k,l} \tag{16}$$

Then, the pairwise similarity matrix for the evidence sources can be obtained as:

$$\mathbf{S} = \begin{bmatrix} 1 & S^{1,2} & \cdots & S^{1,M} \\ S^{2,1} & 1 & \cdots & S^{2,M} \\ \vdots & \vdots & \vdots & \vdots \\ S^{M,1} & S^{M,2} & \cdots & 1 \end{bmatrix}_{M\times M} \tag{17}$$

By summing the elements of each row of the similarity matrix $\mathbf{S}$, the support degree for the k-th evidence source is obtained as:

$$z^k = \sum_{j=1}^{M} S^{j,k}. \, (j = 1, 2, \cdots, M) \tag{18}$$

By normalizing, the basic posterior weight of the k-th data source is obtained as:

$$w_k = \frac{z_k}{\sum_{k=1}^{M} z_k} \tag{19}$$

The prior weights can be obtained through a comprehensive evaluation conducted by domain experts based on multiple aspects of each data source, including testing conditions, data acquisition processes, information credibility, and source characteristics. For M data sources, with prior weights and posterior weights denoted by $\boldsymbol{\lambda} = (\lambda_1, \lambda_2, \cdots, \lambda_M)$ and $\mathbf{w} = (w_1, w_2, \cdots, w_M)$ respectively, we use the multiplicative integration method [22] to determine the comprehensive weight of the k-th data source as:

$$\omega_k = \frac{\lambda_k w_k}{\sum_{k=1}^{M} \lambda_k w_k} \tag{20}$$

3.4 Multi-Source Heterogeneous Degradation Data Fusion

After obtaining the comprehensive weights of multi-source data, in the case involving small-sample data sources, the comprehensive weight-based weighted fusion method is adopted to fuse the data. The main steps are as follows:

First, unified representation of multi-source data using evidence theory:

- Small-sample data (with sample size less than 30) are directly represented as evidence bodies, without any subjective assumptions or parameter estimation;
- For large-sample data, their probability distribution functions are first constructed and then transformed into evidence bodies using the method described in Section 3.2.

Then data fusion is performed based on the comprehensive weights of multi-source data obtained in Section 3.3. Suppose there are M data sources, and after unified representation, each data source has n focal elements, denoted as:

$$\begin{cases} \mathbf{c}^1 = \left[c_1^1, c_2^1, \cdots, c_n^1\right], \text{ where } c_i^1 = \left[y_{(i)}^1, y_{(i+1)}^1\right] \\ \mathbf{c}^2 = \left[c_1^2, c_2^2, \cdots, c_n^2\right], \text{ where } c_i^2 = \left[y_{(i)}^2, y_{(i+1)}^2\right] \\ \cdots \\ \mathbf{c}^M = \left[c_1^M, c_2^M, \cdots, c_n^M\right]. \text{ Where } c_i^M = \left[y_{(i)}^M, y_{(i+1)}^M\right] \end{cases} \tag{21}$$

And BPAs:

$$m\left(c_i^1\right) = m\left(c_i^2\right) = \cdots m\left(c_i^M\right) \tag{22}$$

According to Section 3.3, the comprehensive weights obtained are:

$$\boldsymbol{\omega} = [\omega_1, \omega_2, \ldots, \omega_M] \tag{23}$$

Using the weighted fusion method, the weighted fusion formula is constructed as follows:

$$y_{(i)} = \omega_1 y^1_{(i)} + \omega_2 y^2_{(i)} + \cdots \omega_M y^M_{(i)} \tag{24}$$

The resulting new sequence $\{y_1, y_2, \cdots y_{n+1}\}$ constitutes a set of updated focal elements obtained through the weighted synthesis of quantiles from each data source at identical cumulative probability levels. By incorporating the informational contributions of all sources, this fused sequence exhibits enhanced robustness compared to quantile sequences derived from any individual source, and can therefore be interpreted as a degradation prediction sequence that integrates multi-source uncertainty information. Let the upper and lower bounds of y_i be denoted by $\overline{y}$ and $\underline{y}$ respectively, and set $h_i = (y_i, y_{i+1}]$, with the corresponding BPA denoted by $m(h_i) = m\left(c_i^1\right) = m\left(c_i^2\right) = \cdots m\left(c_i^M\right)$. Then the belief function and plausibility function of the evidence variable X at time-slice t_j can be obtained as:

$$Bel^{t_j}(x) = \begin{cases} \sum\limits_{y_{i+1}<x} m(h_i), & x \in \left[\underline{y}, \overline{y}\right] \\ 1, & x > \overline{y} \\ 0. & x < \underline{y} \end{cases} \tag{25}$$

$$Pl^{t_j}(x) = \begin{cases} \sum\limits_{y_i<x} m(h_i), & x \in \left[\underline{y}, \overline{y}\right] \\ 1, & x > \overline{y} \\ 0. & x < \underline{y} \end{cases} \tag{26}$$

4 Interval Reliability Assessment Based on Wiener Process Using Fused Time-Slice Data

The fused data only represent product performance degradation at discrete time-slices. To further evaluate the degradation process and product reliability, it is necessary to process the fused degradation data across multiple time points. The degradation increments of the fused data at different time points exhibit randomness, which conforms to a continuous-time stochastic process. Traditional data processing methods often neglect or underestimate the randomness and uncertainty in the data. Therefore, the Wiener process is selected to model the degradation data, as it can effectively account for uncertainty and more comprehensively reflect the range of possible outcomes. This section presents the interval reliability assessment framework based on the Wiener process using the fused time-slice degradation data. Building upon the P-Box representations obtained from the previous data fusion stage, this part focuses on modeling the temporal evolution of degradation and further quantifying product reliability in an interval form.

4.1 Theory of the Wiener Process

The Wiener process is a stochastic process with independent and stationary increments, commonly used to describe continuous-time random phenomena. In reliability engineering, the Wiener process is widely employed to characterize the stochastic evolution of product performance degradation.

In practical engineering applications, the Wiener process with drift is often used to describe the degradation process $X(t)$ [23]:

$$X(t) = x_0 + \mu t + \sigma B(t) \tag{27}$$

where μ is the drift parameter, $\sigma > 0$ is the diffusion parameter, and $B(t)$ is the standard Brownian motion. It also has the following properties:

- Degradation increments in any two non-overlapping time intervals are independent of each other.
- The degradation increment over any time interval follows a normal distribution:

$$X(t + \Delta t) - X(t) \sim \mathcal{N}\left(\mu \Delta t, \sigma^2 \Delta t\right) \tag{28}$$

4.2 Parameter Estimation of the Model Driven by Fused Data

In practical applications, raw multi-source data often have different sampling frequencies. To facilitate fusion and modeling, all data sources are first aligned to a unified sampling time $t_0, t_1, \cdots, t_T$ through interpolation or resampling methods. After the data fusion described in Section 3, P-box data with upper and lower bounds are obtained at each time-slice. The characteristics of degradation data are embodied in the multiple sets of P-box data obtained at different time points. Therefore, for the P-box data at each time-slice, N points are respectively taken between 0 and 1 using equally spaced probability sampling, with the cumulative probability corresponding to the i-th point being:

$$cp_j = \frac{j}{N+1}. j = 1, 2 \ldots N \tag{29}$$

For each probability level cp_j, the corresponding lower bound $x_j^L(t_i)$ and upper bound $x_j^U(t_i)$ are extracted from the P-box at that time-slice (as shown in Fig. 4), forming an interval $\left(x_j^L(t), x_j^U(t)\right)$. This interval characterizes the possible range of degradation values at cumulative probability level cp_j, reflecting the uncertainty of degradation at that time-slice. Furthermore, we can obtain the lower bound degradation matrix $X^L \in \mathbb{R}^{N\times(T+1)}$ and upper bound degradation matrix $X^U \in \mathbb{R}^{N\times(T+1)}$ of the product:

$$X^L = \begin{bmatrix} x_1^L(t_0) & x_1^L(t_1) & \cdots & x_1^L(t_T) \\ x_2^L(t_0) & x_2^L(t_1) & \cdots & x_2^L(t_T) \\ \vdots & \vdots & \ddots & \vdots \\ x_N^L(t_0) & x_N^L(t_1) & \cdots & x_N^L(t_T) \end{bmatrix}; X^U = \begin{bmatrix} x_1^U(t_0) & x_1^U(t_1) & \cdots & x_1^U(t_T) \\ x_2^U(t_0) & x_2^U(t_1) & \cdots & x_2^U(t_T) \\ \vdots & \vdots & \ddots & \vdots \\ x_N^U(t_0) & x_N^U(t_1) & \cdots & x_N^U(t_T) \end{bmatrix}. \tag{30}$$

Let the time-slice index be $i = 0, 1, \cdots, T$, corresponding to time t_i, with the time step $\Delta t = t_{i+1} - t_i$ being constant. The lower bound sample vector at each time-slice is $L_i = \left[L_i^{(1)}, L_i^{(2)}, \cdots, L_i^{(N)}\right]^T$, and the upper bound sample vector is $U_i = \left[U_i^{(1)}, U_i^{(2)}, \cdots, U_i^{(N)}\right]^T$.

To use the Wiener process to describe the dynamic evolution of degradation, it is necessary to verify that its increments satisfy the assumption of normal distribution. First, calculate the lower bound increments between adjacent time-slices:

$$\Delta L_i{}^{(k)} = L_{i+1}{}^{(k)} - L_i^{(k)}, \quad i = 0, \ldots, T-1, k = 1, \ldots, N \tag{31}$$

All lower bound increments are pooled into a set $\{\Delta L_m\}_{m=1}^{K}$, where $K = T \times N$. The Kolmogorov-Smirnov (K-S) test is used to perform a normality test on this set. If the test result does not reject the null hypothesis ($p > 0.05$), the lower bound increments can be considered to follow a normal distribution, which is consistent with the basic assumptions of the Wiener process. Similarly, the same normality test is performed on the upper bound increments $\Delta U_i{}^{(k)} = U_{i+1}{}^{(k)} - U_i^{(k)}$.

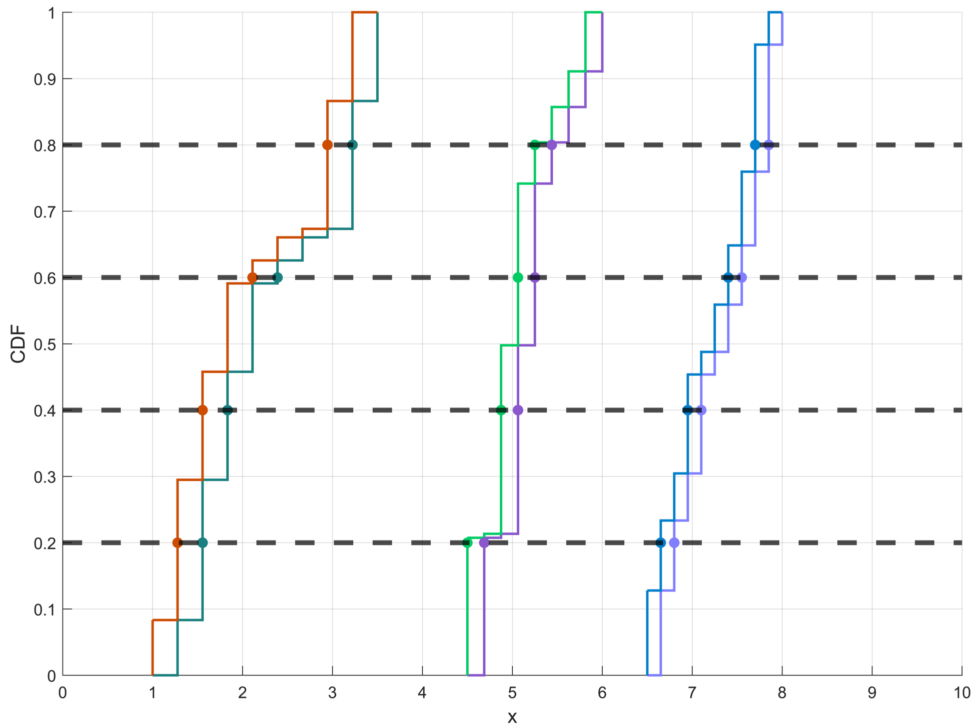

Figure 4: Illustration of equally spaced probability sampling.

Under the premise that the normality assumption of increments holds, the parameters of the lower bound and upper bound Wiener processes are estimated. Let the sample mean and sample variance of the increments be denoted respectively as:

$$\begin{cases} \mu_{\Delta L} = \frac{1}{K}\sum_{i=1}^{K}\Delta L_i; \sigma_{\Delta L}^2 = \frac{1}{K-1}\sum_{i=1}^{K}\left(\Delta L_i - \mu_{\Delta L}\right)^2 \\ \mu_{\Delta U} = \frac{1}{K}\sum_{i=1}^{K}\Delta U_i; \sigma_{\Delta U}^2 = \frac{1}{K-1}\sum_{i=1}^{K}\left(\Delta U_i - \mu_{\Delta U}\right)^2 \end{cases} \tag{32}$$

Based on the incremental properties of the Wiener process, the drift parameter and diffusion parameter per unit time are:

$$\mu_L = \frac{\hat{\mu}_{\Delta L}}{\Delta t}; \sigma_L^2 = \frac{\hat{\sigma}_{\Delta L}^2}{\Delta t}; \mu_U = \frac{\hat{\mu}_{\Delta U}}{\Delta t}; \sigma_U^2 = \frac{\hat{\sigma}_{\Delta U}^2}{\Delta t}. \tag{33}$$

Then, the initial distribution parameters of the upper bound process and lower bound process at initial time t_0 are calculated as:

$$\overline{L}_{t_0} = \frac{1}{N}\sum_{i=1}^{N} L_{t_0}^{(i)}; s_{L,t_0}^2 = \frac{1}{N-1}\sum_{i=1}^{N}\left(L_{t_0}^{(i)} - \overline{L}_{t_0}\right)^2;$$
$$\overline{U}_{t_0} = \frac{1}{N}\sum_{i=1}^{N} U_{t_0}^{(i)}; s_{U,t_0}^2 = \frac{1}{N-1}\sum_{i=1}^{N}\left(U_{t_0}^{(i)} - \overline{U}_{t_0}\right)^2. \tag{34}$$

Thus, two Wiener processes, namely the upper bound process and the lower bound process, are obtained respectively:

$$\begin{aligned} X_L(t) &= X_L(t_0) + \mu_L(t - t_0) + \sigma_L(B(t) - B(t_0)), X_L(t_0) \sim \mathcal{N}\left(\overline{L}_{t_0}, s^2_{L,t_0}\right) \\ X_U(t) &= X_U(t_0) + \mu_U(t - t_0) + \sigma_U(B(t) - B(t_0)). X_U(t_0) \sim \mathcal{N}\left(\overline{U}_{t_0}, s^2_{U,t_0}\right) \end{aligned} \tag{35}$$

4.3 Interval Reliability Assessment

In reliability engineering, product lifetime is often defined as the time when the degradation quantity first crosses the failure threshold, namely the first passage time. For the case where the degradation quantity increases, let the failure threshold be X_{th}, then the product lifetime is defined as [24]:

$$T_f = \inf\{t \geq t_0 : X(t) \geq X_{th}\} \tag{36}$$

The reliability function $R(t) = P\left(T_f > t\right)$ represents the probability that the product has not failed before time t. When the degradation process is a Wiener process and the initial value is a deterministic value x_0, the first passage time follows an inverse Gaussian distribution, and the reliability function has an analytical expression [25]:

$$R(t) = \Phi\left(\frac{X_{th} - x_0 - \mu(t - t_0)}{\sigma\sqrt{t - t_0}}\right) - \exp\left(\frac{2\mu(X_{th} - x_0)}{\sigma^2}\right)\Phi\left(\frac{-X_{th} + x_0 - \mu(t - t_0)}{\sigma\sqrt{t - t_0}}\right) \tag{37}$$

where $\Phi(\cdot)$ is the standard normal cumulative distribution function.

For the case where the degradation quantity decreases, let the failure threshold be X_{th}, then the product lifetime is defined as:

$$T_f = \inf\{t \geq t_0 : X(t) \leq X_{th}\} \tag{38}$$

Its reliability function is:

$$R(t) = \Phi\left(\frac{-X_{th} + x_0 + \mu(t - t_0)}{\sigma\sqrt{t - t_0}}\right) - \exp\left(\frac{2\mu(X_{th} - x_0)}{\sigma^2}\right)\Phi\left(\frac{X_{th} - x_0 + \mu(t - t_0)}{\sigma\sqrt{t - t_0}}\right) \tag{39}$$

Using the mean of the initial distribution to approximate the initial degradation value of the product, and then substituting the corresponding parameters $\left(\mu_L, \sigma_L, \overline{L}_{t_0}\right)$ and $\left(\mu_U, \sigma_U, \overline{U}_{t_0}\right)$, the reliability functions of the lower bound process and upper bound process are obtained as $R_L(t)$ and $R_U(t)$:

- When the degradation quantity increases:

$$\begin{cases} R_L(t) = \Phi\left(\frac{X_{th} - \overline{L}_{t_0} - \mu_L(t - t_0)}{\sigma_L\sqrt{t - t_0}}\right) - \exp\left(\frac{2\mu_L\left(X_{th} - \overline{L}_{t_0}\right)}{\sigma_L^2}\right)\Phi\left(\frac{-X_{th} + \overline{L}_{t_0} - \mu_L(t - t_0)}{\sigma_L\sqrt{t - t_0}}\right) \\ R_U(t) = \Phi\left(\frac{X_{th} - \overline{U}_{t_0} - \mu_U(t - t_0)}{\sigma_U\sqrt{t - t_0}}\right) - \exp\left(\frac{2\mu_U\left(X_{th} - \overline{U}_{t_0}\right)}{\sigma_U^2}\right)\Phi\left(\frac{-X_{th} + \overline{U}_{t_0} - \mu_U(t - t_0)}{\sigma_U\sqrt{t - t_0}}\right) \end{cases} \tag{40}$$

- When the degradation quantity decreases:

$$\begin{cases} R_L(t) = \Phi\left(\frac{\overline{L}_{t_0} - X_{th} + \mu_L(t - t_0)}{\sigma_L\sqrt{t - t_0}}\right) - \exp\left(\frac{2\mu_L\left(X_{th} - \overline{L}_{t_0}\right)}{\sigma_L^2}\right)\Phi\left(\frac{X_{th} - \overline{L}_{t_0} + \mu_L(t - t_0)}{\sigma_L\sqrt{t - t_0}}\right) \\ R_U(t) = \Phi\left(\frac{\overline{U}_{t_0} - X_{th} + \mu_U(t - t_0)}{\sigma_U\sqrt{t - t_0}}\right) - \exp\left(\frac{2\mu_U\left(X_{th} - \overline{U}_{t_0}\right)}{\sigma_U^2}\right)\Phi\left(\frac{X_{th} - \overline{U}_{t_0} + \mu_U(t - t_0)}{\sigma_U\sqrt{t - t_0}}\right) \end{cases} \tag{41}$$

When the degradation quantity increases, since the lower bound process $X_L(t)$ represents a superior degradation path (with smaller degradation values), its first passage time is longer, so $R_U(t) \le R_L(t)$. Therefore, the true value of product reliability is covered by the interval $[R_U(t), R_L(t)]$. When the degradation quantity decreases, $R_L(t) \le R_U(t)$, and thus the true value of product reliability lies in the interval $[R_L(t), R_U(t)]$.

4.4 Area Metric for Fusion Effect Evaluation

To accurately illustrate the effectiveness of the fusion results, we define an area metric for quantitative analysis. The area metric method was first proposed by American scholars Ferson and Oberkampf [26,27]. It is a validation metric based on the distance between probability distributions, primarily used in the field of modeling and simulation. Let the reliability function of the upper bound process obtained from Section 4.3 be $R^U(t)$ and that of the lower bound process be $R^L(t)$. By drawing on the area metric, the uncertainty of the fusion results in this paper (the area of the shaded region in Fig. 5) is defined as:

$$A\left(R^U(t), R^L(t)\right) = \int_{-\infty}^{+\infty} \left|R^U(t) - R^L(t)\right| dt \tag{42}$$

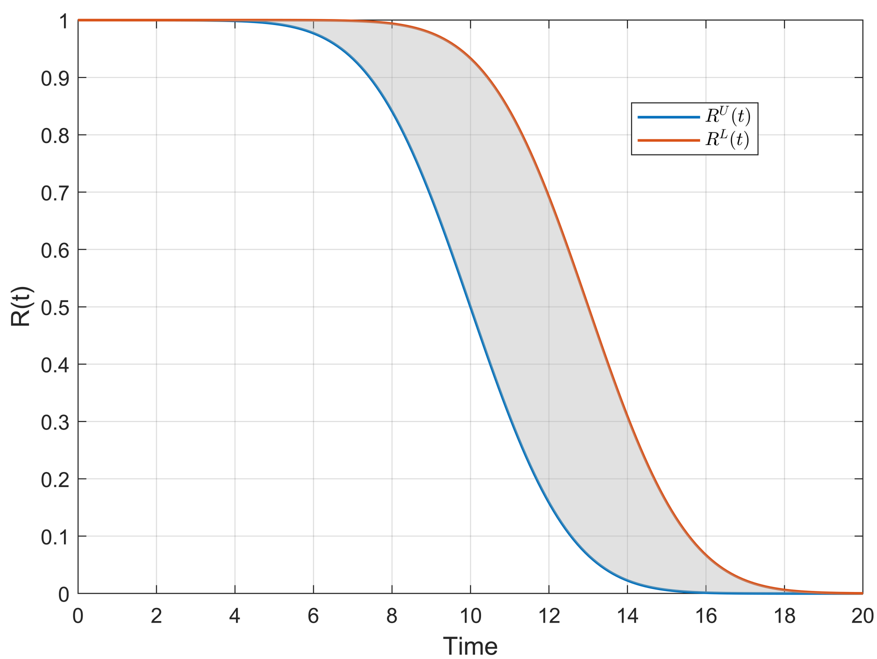

Figure 5: Illustration of the area metric method based on probability distribution distance.

Furthermore, when the two functions obtained from data fusion are closer, the area metric is smaller, indicating a narrower range of reliability estimation at a given time point and thus lower uncertainty. Suppose that by directly solving the distribution parameters from different data sources, we obtain single reliability functions $R_1(t), R_2(t), \cdots, R_M(t)$ from different data sources. Taking $R_{\min}(t) = \min_{i\in\{1,2\cdots M\}} R_i(t)$, $R_{\max}(t) = \max_{i\in\{1,2\cdots M\}} R_i(t)$:

$$A\left(R_{\max}(t), R_{\min}(t)\right) = \int_{-\infty}^{+\infty} \left|R_{\max}(t) - R_{\min}(t)\right| dt \tag{43}$$

If $A\left(R^U(t), R^L(t)\right) < A\left(R_{\max}(t), R_{\min}(t)\right)$, it indicates that the proposed method reduces the uncertainty introduced by information from different data sources.

Building upon the idea of the area metric defined above, to more accurately measure the effectiveness of the fusion method, it is necessary to compare the area metric values between the reliability functions of the fused data and the true reliability function of the sample. Let the true reliability function be $R^{\text{true}}(t)$. When the fusion method is effective, the differences between the fused data reliability functions $R^U(t)$ and $R^L(t)$ and the true reliability function $R^{\text{true}}(t)$ should be small. Therefore, we consider calculating the area metric values between $R^U(t)$ and $R^{\text{true}}(t)$, and between $R^L(t)$ and $R^{\text{true}}(t)$, respectively:

$$\begin{cases} A\left(R^U(t), R^{\text{true}}(t)\right) = \int_{-\infty}^{+\infty} \left|R^U(t) - R^{\text{true}}(t)\right| dt \\ A\left(R^L(t), R^{\text{true}}(t)\right) = \int_{-\infty}^{+\infty} \left|R^L(t) - R^{\text{true}}(t)\right| dt \end{cases} \tag{44}$$

Similarly, the area metric values between the reliability functions obtained from the comparison method and the true reliability function are calculated as comparative data. By definition, a smaller area metric value indicates better model estimation. In practical numerical implementation, the integration is performed over a sufficiently large finite interval, beyond which the reliability value becomes negligibly small. Therefore, the numerical difference between the truncated computation and the infinite-domain formulation is generally insignificant.

5 Case Analysis

We use two cases to verify the effectiveness and engineering applicability of the proposed method. Section 5.1 constructs test samples with different distribution parameters and sample sizes through simulation experiments to verify the effectiveness of the method, and compares it with the Bayesian fusion method [13] and Yang's fusion method [12] as the control groups. Section 5.2 evaluates actual test data of gyro components in the attitude control system of a Geostationary Earth Orbit (GEO) satellite, with different scales and populations, primarily to verify the applicability and effectiveness of the proposed method in practical engineering applications. The main calculation results are presented.

5.1 Simulation Case Study

To evaluate the effectiveness of the proposed method, we set up three Wiener processes: $X_1(t), X_2(t), X_3(t)$, representing the true degradation processes of the same product from three different data sources, with parameters shown in Table 1. We designate $X_1(t)$ as the actual product degradation process and use it as the benchmark process. It can be seen from the table that the drift parameter of $X_2(t)$ is the same as that of the benchmark process, but the diffusion parameter is slightly different. The diffusion parameter of $X_3(t)$ is the same as that of the benchmark process, but its drift parameter is slightly larger than that of the benchmark process. Each sample path is sampled at a fixed time interval $\Delta t = 1$, with a total of 5 sampling points. The sample sizes for each process are 7, 35, and 30, respectively. The data are shown in Figs. 6–8. Let the first data set D_1 be actual product performance degradation data, the second data set D_2 be semi-simulation performance degradation data, and the third data set D_3 be numerical simulation performance degradation data.

Table 1: Table of parameters for stochastic processes.

Parameter	$X_1(t)$	$X_2(t)$	$X_3(t)$
μ	10	10	14
σ	4	7	4

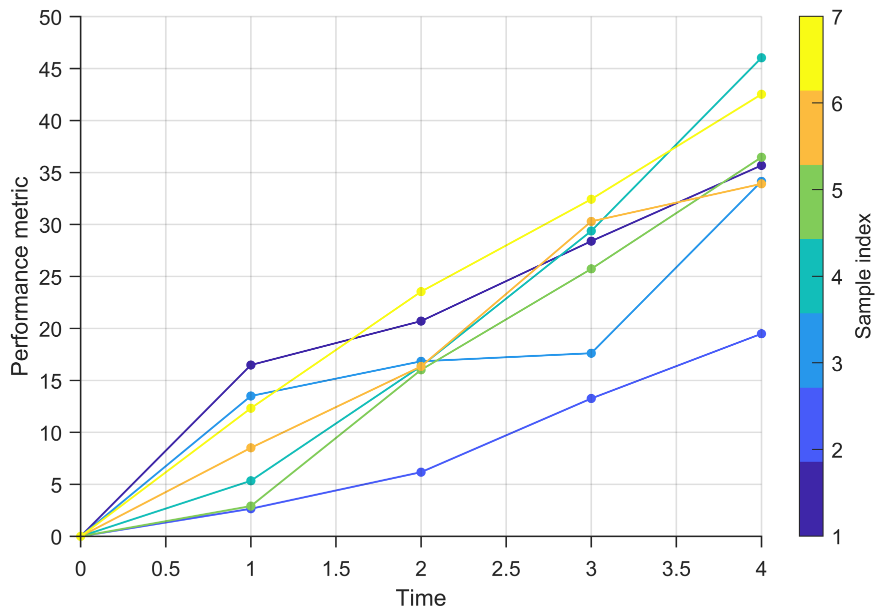

Figure 6: Sampling data of Wiener process $X_1(t)$.

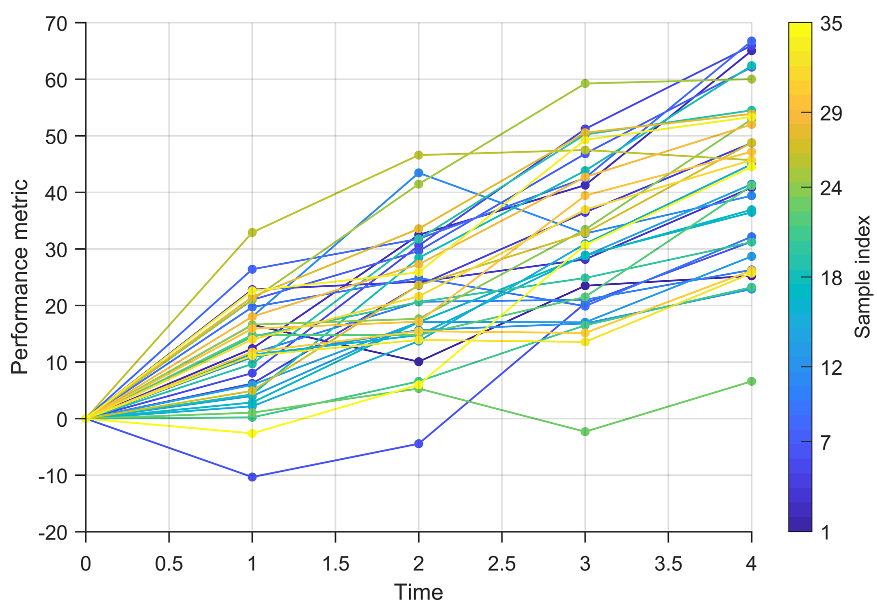

Figure 7: Sampling data of Wiener process $X_2(t)$.

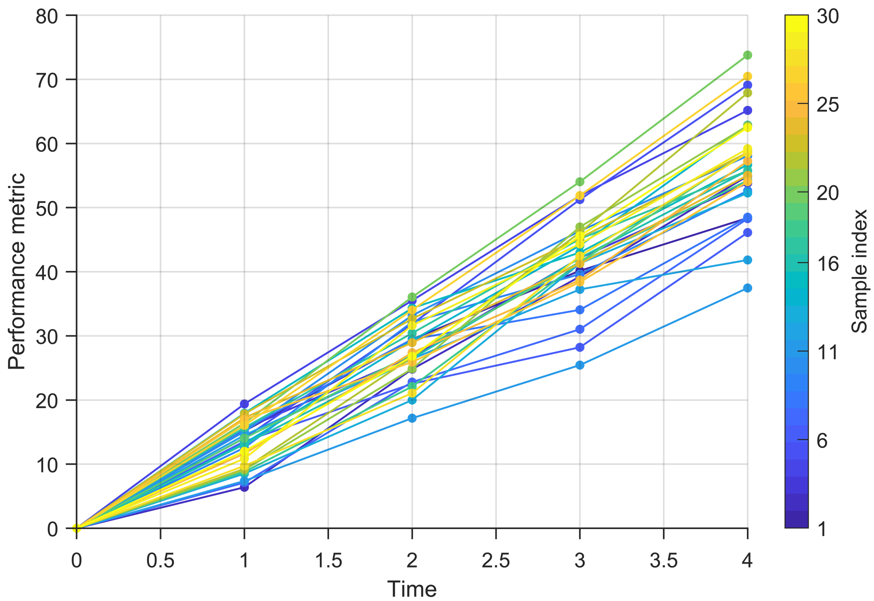

Figure 8: Sampling data of Wiener process $X_3(t)$.

Assuming the failure threshold of the product is 40, data source D_1 has a small sample size and its uncertainty is characterized using the method described in Section 3.1. For the other two data sources, normality tests are first performed (as shown in Table 2), followed by parameter estimation using the maximum likelihood estimation method. The features of data sources D_2 and D_3 are then extracted. Taking the prior weights as $\lambda = (0.5, 0.3, 0.2)$, and then combining with the content in Section 3.3, the comprehensive weights for each time-slice are shown in Table 3.

Table 2: p Values of each data soures.

Data Source	$\Delta X(t_2)$	$\Delta X(t_3)$	$\Delta X(t_4)$	$\Delta X(t_5)$
Source 2	0.5000	0.5000	0.5000	0.2891
Source 3	0.3142	0.4361	0.5000	0.0601

Table 3: Comprehensive weights for each time-slice.

Data Source	ω^{t_1}	ω^{t_2}	ω^{t_3}	ω^{t_4}	ω^{t_5}
Source 1	0.3333	0.5523	0.4994	0.5282	0.5287
Source 2	0.3333	0.2898	0.3476	0.3363	0.3381
Source 3	0.3333	0.1578	0.1530	0.1355	0.1332

Then, after performing weighted fusion on the data from the three sources, the quantile matrix is obtained (each column represents a time-slice):

$$Y=\begin{bmatrix}0.0000 & 0.2997 & 4.1652 & 12.6848 & 22.2287\\ 0.0000 & 3.5712 & 7.3297 & 16.0263 & 27.0880\\ 0.0000 & 7.0113 & 12.5838 & 23.0717 & 34.2716\\ 0.0000 & 9.8800 & 17.7304 & 28.8929 & 38.7856\\ 0.0000 & 11.8587 & 21.4436 & 33.0022 & 42.4176\\ 0.0000 & 13.9876 & 25.1930 & 36.7610 & 46.7911\\ 0.0000 & 15.6192 & 28.1083 & 39.9893 & 51.7079\\ 0.0000 & 18.8253 & 35.3685 & 48.8531 & 60.7395\end{bmatrix}.$$

Since the degradation amount at the initial time is 0, the first column of the BPA vector takes a uniform value, and the quantile obtained through weighting is also 0.

Ten points are uniformly taken in the interval $[0,1]$, the upper and lower bound data matrices are extracted, and then parameter estimation is performed to obtain two Wiener processes: the upper bound process and the lower bound process.

$$\begin{aligned}X_L(t) &= 9.6312t + 10.6175B(t),\\ X_U(t) &= 10.5941t + 10.4574B(t).\end{aligned} \tag{45}$$

Then, the reliability functions of the upper bound process and lower bound process are obtained (as shown in Fig. 9):

$$\begin{aligned}R_L(t) &= \Phi\left(\frac{40-9.6312t}{3.2585\sqrt{t}}\right) - \exp\left(\frac{2\times 9.6312\times 40}{10.6175}\right)\Phi\left(\frac{-40-9.6312t}{3.2585\sqrt{t}}\right),\\ R_U(t) &= \Phi\left(\frac{40-10.5941t}{3.2338\sqrt{t}}\right) - \exp\left(\frac{2\times 10.5941\times 40}{10.4574}\right)\Phi\left(\frac{-40-10.5941t}{3.2338\sqrt{t}}\right).\end{aligned} \tag{46}$$

Parameter estimation of the Wiener process was performed separately for the three data sources, and the obtained reliability curves are shown in Fig. 10. Then the area metric values $A\left(R^U(t), R^L(t)\right) = 0.3774$ and $A\left(R_{\max}(t), R_{\min}(t)\right) = 1.6275$ were calculated. This indicates that the proposed method reduces the uncertainty from different data sources.

The parameter estimates of D_2 and D_3 are used as prior information, and then the posterior is updated based on the data of D_1 to obtain parameter estimates of the drift and diffusion parameters, thereby obtaining the reliability function based on the Bayesian method (as shown in Fig. 9):

$$R_B(t) = \Phi\left(\frac{40-10.5918t}{5.8339\sqrt{t}}\right) - \exp\left(\frac{2\times 10.5918\times 40}{34.0345}\right)\Phi\left(\frac{-40-10.5918t}{5.8339\sqrt{t}}\right). \tag{47}$$

Yang's fusion method is also shown in Fig. 9.

The area metric values between the true reliability curve and those obtained by the proposed method and control methods were calculated respectively: $A\left(R^L(t), R^{\text{true}}(t)\right) = 0.1704$, $A\left(R^U(t), R^{\text{true}}(t)\right) = 0.2367$, $A\left(R_B(t), R^{\text{true}}(t)\right) = 0.3088$, $A\left(R_Y(t), R^{\text{true}}(t)\right) = 0.5435$. Area metric values of the proposed method are significantly smaller than those of the comparison method, and it can be seen from Fig. 9 that the true reliability curve is mostly enveloped within our upper and lower bound reliability functions.

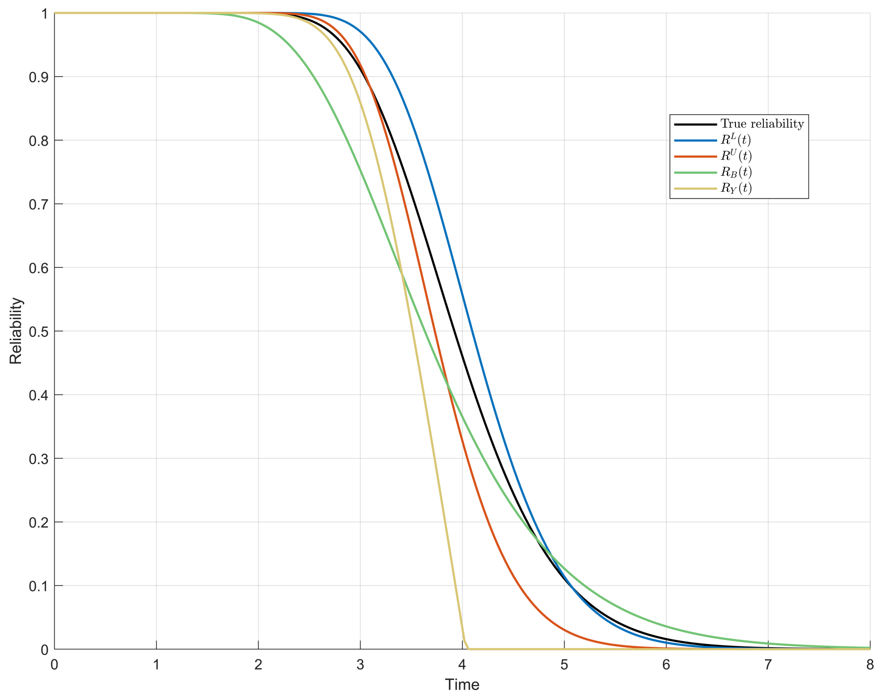

Figure 9: Comparison of reliability curves for different methods.

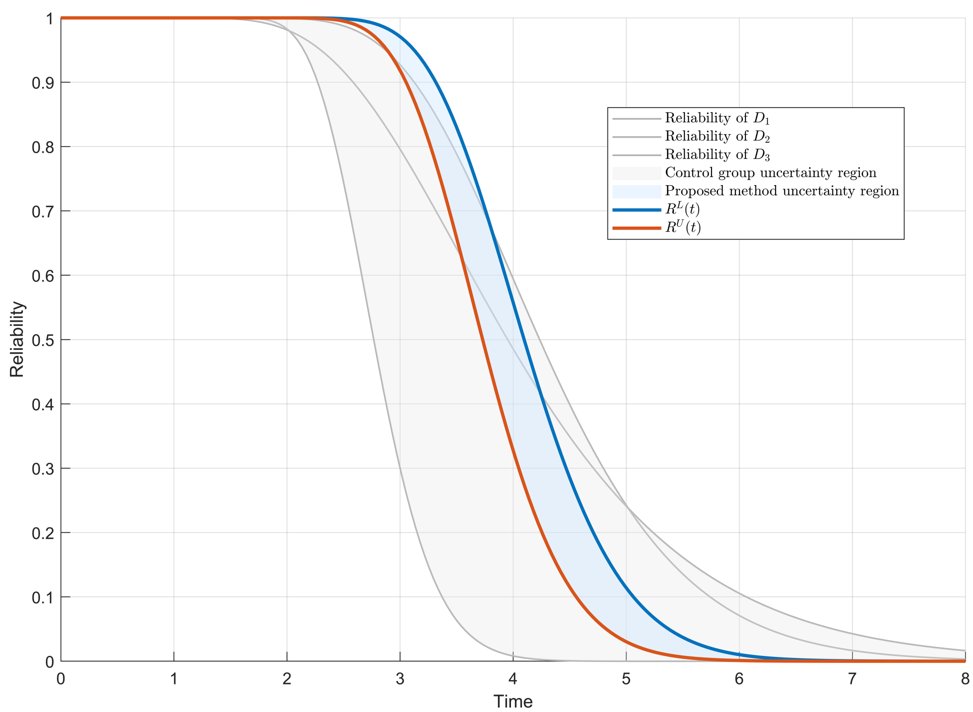

Figure 10: Comparison of areas of uncertainty.

Next, multiple sampling runs were conducted to verify the robustness of the proposed method, with the results shown in Table 4. It can be seen from the table that the proposed method exhibits satisfactory robustness, and the resulting reliability curves are closer to the true reliability curve.

Table 4: Table of results from multiple samples using different fusion methods.

Sample Number	**1**	**2**	**3**	**4**	**5**
$A\left(R^{L}(t), R^{\text{true}}(t)\right)$	0.1813	0.2230	0.2265	0.2074	0.1051
$A\left(R^{U}(t), R^{\text{true}}(t)\right)$	0.3012	0.3658	0.2348	0.2572	0.3354
$A\left(R_{B}(t), R^{\text{true}}(t)\right)$	0.3180	0.3985	0.3708	0.3477	0.4350
$A\left(R_{Y}(t), R^{\text{true}}(t)\right)$	0.4765	0.3705	0.3479	0.4258	0.4561

The three fusion approaches differ primarily in the stage at which they handle uncertainty. In the Bayesian approach, auxiliary data sources directly inform prior distribution estimation, allowing uncertainties and biases in the original data to propagate continuously into the posterior. Consequently, estimation accuracy depends heavily on the reliability of the prior information. The method of Zhang et al. [14] mitigates this issue partially by first performing maximum likelihood estimation (MLE) separately for each source and then conducting fusion. This strategy can extract common characteristics across sources to improve robustness. However, because estimation errors from individual datasets are already embedded in the MLE-derived parameters, the subsequent fusion cannot fully eliminate these propagated uncertainties. The proposed framework addresses this limitation by performing weighted fusion at the data level, prior to stochastic degradation modelling and it's parameter estimation. This design attenuates the influence of low-credibility or high-uncertainty sources during fusion itself, thereby reducing the propagation of source-specific uncertainty into downstream parameter estimation and reliability assessment. Under the multi-source heterogeneous degradation scenarios examined here, the proposed method demonstrates favourable robustness and reliability assessment performance relative to both the Bayesian-based approach and the parameter-level fusion strategy of Yang et al. [14].

5.2 Engineering Case Study

The gyro components in a satellite serve as attitude sensors and stabilizers. They not only monitor the satellite's rotation speed and spatial orientation in real time, but also control the satellite to always point toward the target through feedback signals. Combined with related equipment, they enable autonomous navigation and reduce dependence on the ground. When satellite gyro components operate in space along with the satellite, they are affected by extreme space environments such as radiation and temperature, which accelerates their aging. Therefore, understanding the performance degradation and reliability evolution patterns of satellite gyro components is crucial for the stable operation of the satellite.

A comprehensive evaluation is performed on the gyro components within the attitude control system of a geostationary Earth orbit (GEO) satellite. The critical performance metric for these components is the gyro zero-bias drift; failure occurs when this drift exceeds the threshold of 0.05°/h, triggering an automatic redundancy switch. Given the limited sample size and short operational history of new gyro components during actual in-orbit service, the dataset assembled for this case study comprises three distinct sources: (1) ground-based accelerated aging test data, (2) real-time satellite on-orbit data, and (3) historical degradation records from gyro components belonging to the same production batch. Each data source exhibits inherent characteristics that must be considered during fusion: the accelerated aging data are subject to conversion errors when extrapolated to in-orbit conditions; the on-orbit data offer high temporal relevance yet contain considerable measurement noise; and the historical batch data provide robust statistical properties but originate from somewhat divergent operational environments. Based on comprehensive expert evaluation, prior weights of 0.3, 0.5, and 0.2 are assigned to the accelerated aging data, on-orbit data, and historical batch data, respectively. The fusion of these three complementary sources leverages their respective strengths to yield a more accurate characterization of the underlying degradation process.

Ground-based accelerated aging tests were conducted on them, with an acceleration factor of 9.8. The measured degradation data, with a sample size of 7, a test interval of 1 month, and a total duration of 10 months, are shown in Fig. 11.

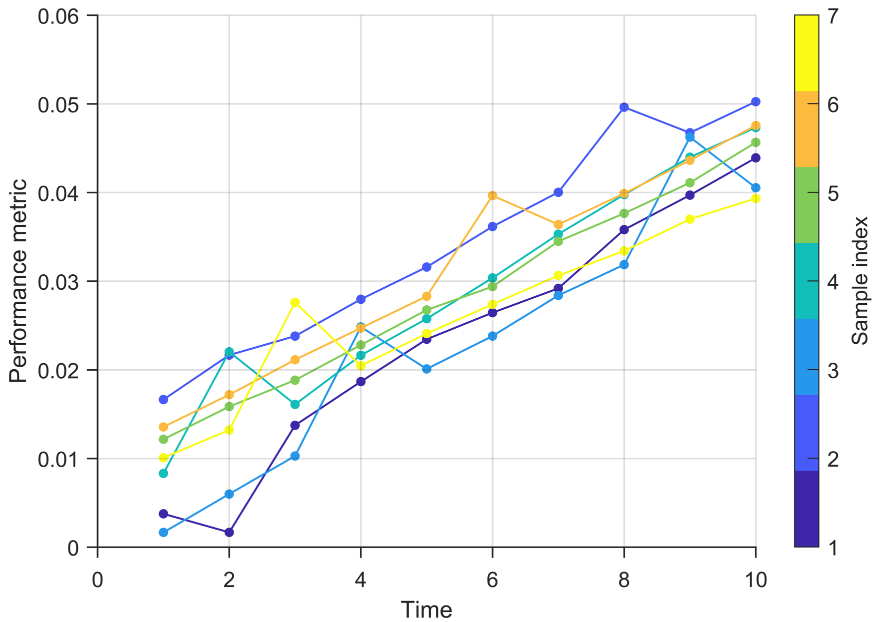

Figure 11: Degradation curves from 10-month ground-based accelerated aging tests.

Concurrently, monthly monitoring data for the first five years after satellite launch were measured. Due to radiation effects causing data jumps, the measured degradation data, with a sample size of 13, a monitoring interval of 3 months, and a total duration of 5 years, are shown in Fig. 12.

The historical data of gyro components from the same batch in this attitude control system are: a sample size of 27, a test interval of 3 months, and a total duration of 5 years, as shown in Fig. 13.

In the ground-based accelerated tests and on-orbit telemetry, data jumps occurred due to radiation effects. The interpolation method using the mean of adjacent values was employed for interpolation. After removing and correcting outliers, the degradation curves for the ground-based accelerated tests and on-orbit telemetry were obtained as shown in Fig. 14.

Since the ground-based accelerated tests were conducted at monthly intervals with a 9.8-fold acceleration factor, while the on-orbit telemetry and historical degradation data from the same satellite batch were collected at trimonthly intervals, the degradation rate of the ground-based accelerated tests was first converted to the normal degradation rate. Then, cubic spline interpolation, a commonly used method, was applied to the data. The interpolation results are shown in Fig. 15, which serves as the basis for subsequent data fusion.

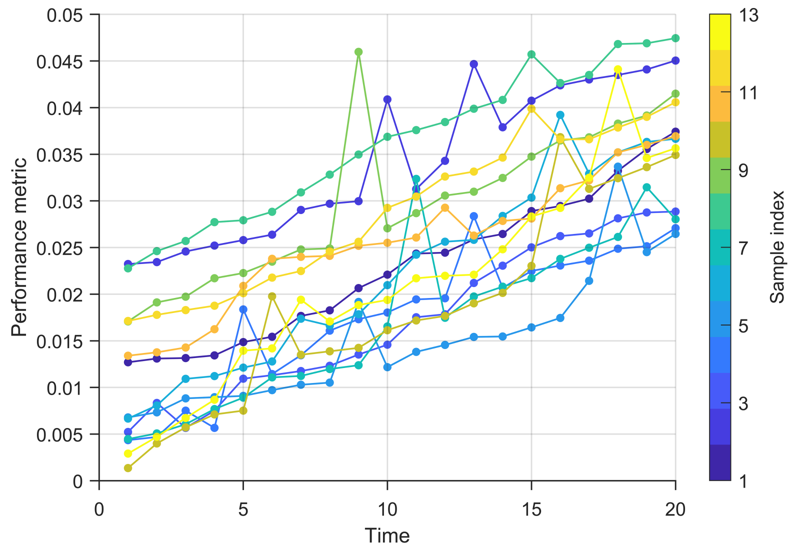

Figure 12: On-orbit telemetry data degradation curves.

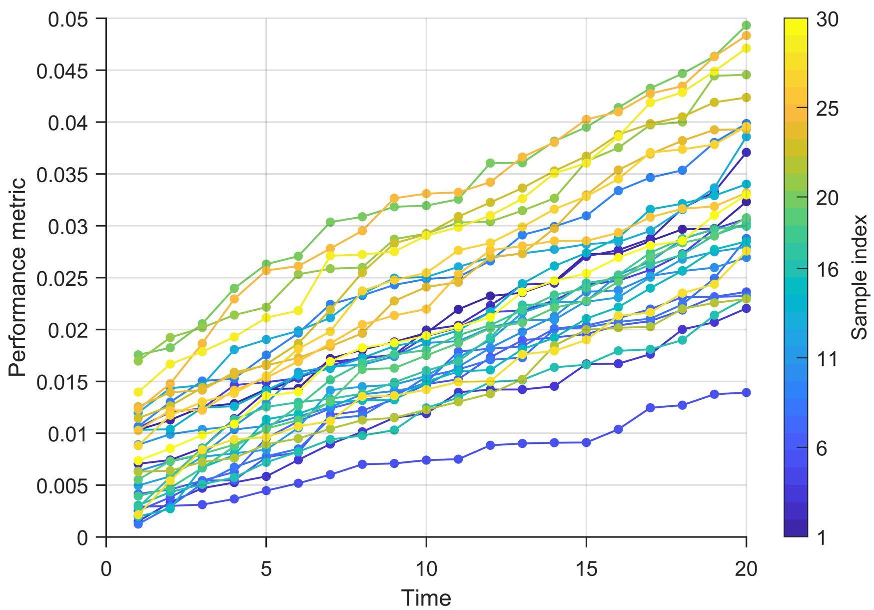

Figure 13: Historical data degradation curves of same-batch satellites.

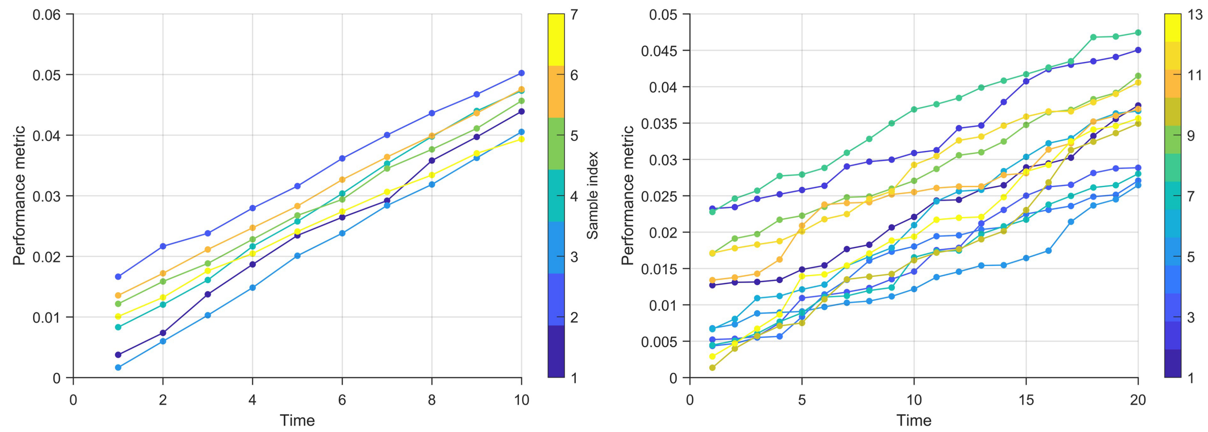

Figure 14: Ground-based accelerated test and on-orbit telemetry degradation curves after outlier removal.

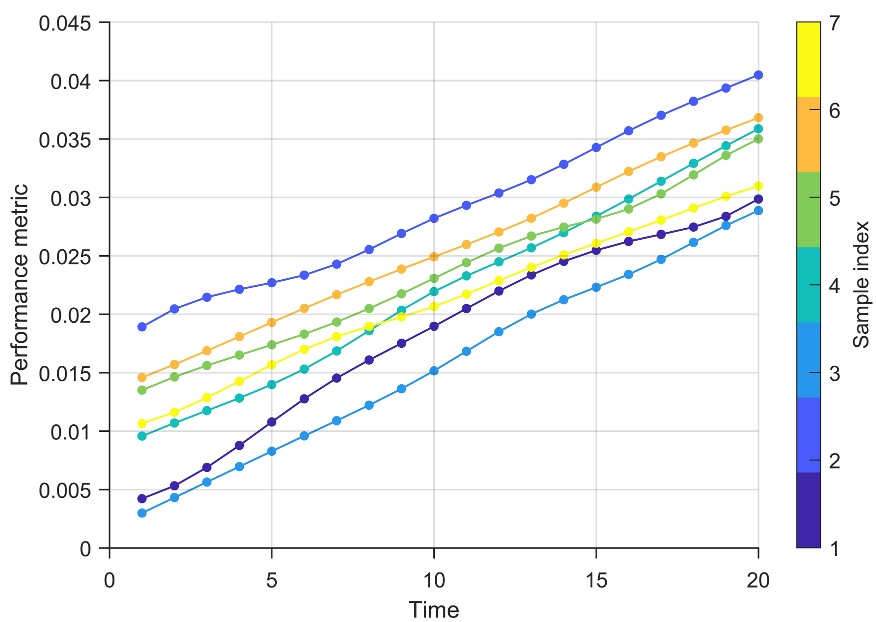

Figure 15: Ground-based accelerated test degradation curves after extended interpolation.

Combining the content in Section 3.3, the comprehensive weight matrix $\boldsymbol{\omega}$ for each time-slice is obtained. Then, after performing weighted fusion on the data from the three sources, the quantile matrix Y and the BPA matrix are obtained. 19 points are uniformly taken in the interval $[0, 1]$ to obtain the upper bound degradation matrix and the lower bound degradation matrix. The K-S test is then used to test the normality of the increments, and the test results indicate that the increments satisfy the normality test. According to the parameter estimation method in Section 4.2, two Wiener processes of the upper bound process and the lower bound process are obtained:

$$\begin{aligned} &X_L(t) = X_L(t_0) + 0.00042t + 0.00015(B(t) - B(t_0)), X_L(t_0) \sim \mathcal{N}(0.0098, 0.000031), \\ &X_U(t) = X_U(t_0) + 0.00043t + 0.00014(B(t) - B(t_0)), X_U(t_0) \sim \mathcal{N}(0.0108, 0.000033). \end{aligned} \tag{48}$$

Substituting the failure threshold, the product reliability is obtained as (shown in Fig. 16):

$$R_L(t) = \Phi\left(\frac{0.05 - 0.0098 - 0.00042t}{0.00015\sqrt{t}}\right) - \exp\left(\frac{2 \times 0.00042\,(0.05 - 0.0098)}{0.00000002}\right)\Phi\left(\frac{-0.05 + 0.0098 - 0.00042t}{0.00015\sqrt{t}}\right),$$

$$R_U(t) = \Phi\left(\frac{0.05 - 0.0108 - 0.00043t}{0.00014\sqrt{t}}\right) - \exp\left(\frac{2 \times 0.00043\,(0.05 - 0.0108)}{0.00000002}\right)\Phi\left(\frac{-0.05 + 0.0108 - 0.0004t}{0.00014\sqrt{t}}\right). \quad (49)$$

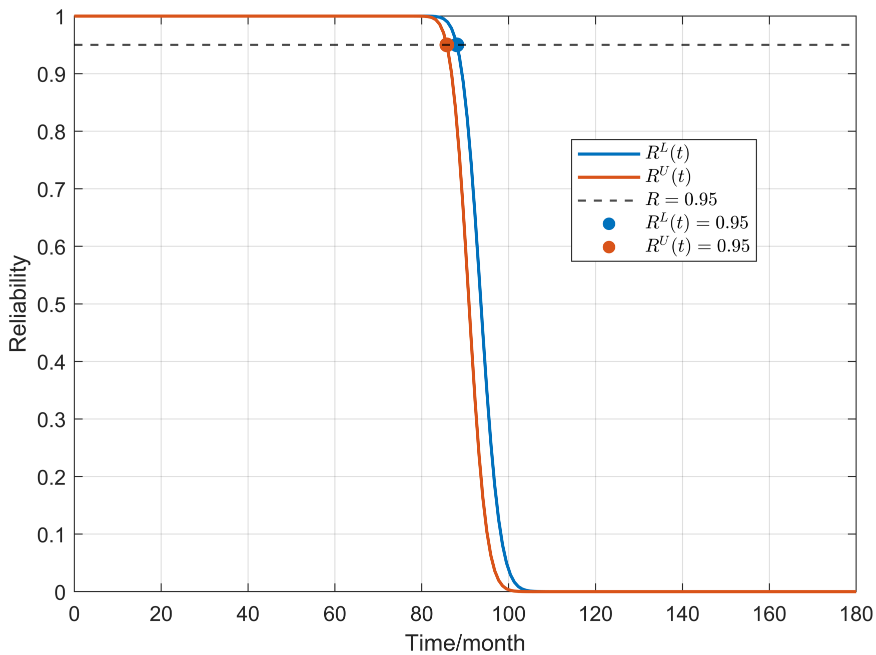

Figure 16: Reliability curves for satellite gyro components following multi-source data fusion.

By calculating the lifetime interval corresponding to a reliability of 0.95 as $[85.8366, 88.0336]$, the reliability curve obtained by the proposed method can effectively quantify uncertainty information and provide a corresponding uncertainty range for the reliability curve. In practical engineering applications, the lower bound of the reliability curve can be selected as the evaluation result, which is more conservative and has higher credibility.

6 Conclusion

This paper addresses the challenge of product degradation prediction when limited experimental test data coexist with abundant semi-simulation and numerical simulation data. A four-step degradation prediction framework is proposed, encompassing data uncertainty characterization, feature extraction through non-uniform probability sampling, comprehensive weight determination for multi-source heterogeneous data, and data-level fusion guided by these weights. The central contribution of this work lies in integrating these steps into a coherent pipeline that reduces uncertainty propagation by performing weighted fusion prior to parameter estimation, rather than relying on conventional approaches that fuse at the parameter or posterior level.

The proposed framework offers several advantages over existing methods. First, by representing small-sample test data as plausibility and belief functions through evidence theory, the method preserves the probability distribution characteristics of the original data. This addresses a limitation of traditional statistical approaches, which often require larger sample sizes to capture the underlying distribution reliably. Second, the non-uniform probability sampling strategy regularizes data sources of vastly different sample sizes into a common feature space, enabling subsequent weight determination and fusion that would otherwise be infeasible when dimensions are mismatched. Third, the comprehensive weighting scheme accounts for epistemic uncertainty arising from sample size disparities, yielding posterior weights that more faithfully reflect the relative informativeness of each source. Fourth, the interval stochastic degradation model based on the Wiener process provides interval-valued reliability estimates that explicitly represent the range of uncertainty under limited samples, rather than relying solely on point estimates. In practical applications, the lower bound of this interval can serve as a conservative reliability estimate, offering clear engineering value for decision-making under uncertainty.

Despite these strengths, the proposed method has limitations that warrant acknowledgement. The framework assumes that all information sources are mutually independent. In practice, this assumption may be violated by common manufacturing defects within the same product batch, systematic biases introduced by shared test instruments or operators, and environmental or temporal correlations among data sources. Furthermore, when multiple sources acquired under off-stress conditions, such as accelerated tests or semi-physical simulation, exhibit systematic biases in the same direction, the distance-based similarity weighting method cannot fully eliminate these biases. Under such conditions, fusion results may deviate from the actual degradation process.

To address these limitations, future work will pursue three directions. First, a data preprocessing mechanism will be designed to evaluate the credibility of each information source based on data completeness, variance stability, and consistency with prior distributions, thereby identifying and removing low-credibility sources before fusion. Second, the method will be extended to incorporate similar product data through similarity weighting based on degradation mechanisms or statistical characteristics, supporting broader small-sample reliability assessment scenarios. Third, a data-fusion-based lifetime prediction methodology will be developed to enhance the applicability of the proposed approach in complex engineering environments.

Acknowledgement: Not applicable.

Funding Statement: This work is financial supported by National Natural Science Foundation of China (grant no. 62374173).

Author Contributions: Ying Yan: Data collection, experimental operation, original manuscript writing, project administration. Yongqiang Yang: Methodology design, result analysis, figure visualization. Cong Jiang: Data sorting, literature investigation, partial discussion revision. Bin Suo: Resource support, experimental verification, formal analysis. Kai Sun: Conceptualization, overall supervision, manuscript review and editing. All authors reviewed and approved the final version of the manuscript.

Availability of Data and Materials: All data generated in this study are derived from our independent experiments. The main data are visualized and presented as scatter plots within the manuscript. The raw experimental data are not publicly available due to relevant research restrictions.

Ethics Approval: Not applicable.

Conflicts of Interest: The authors declare no conflict of interests.

References

1. Gunjan SB, Srinivasu DS, Ramesh Babu N. A new approach for product reliability prediction by considering the production factory lifecycle information. Reliab Eng Syst Saf. 2025;258:110915. doi:10.1016/j.ress.2025.110915.
2. Wang Y, Yang B, Ma J. Bayesian prediction of aerospace system mission reliability with hierarchical and multi-fidelity test data fusion. Reliab Eng Syst Saf. 2026;267(4):111844. doi:10.1016/j.ress.2025.111844.
3. Kang W, Tian Y, Xu H, Wang D, Zheng H, Zhang M, et al. Reliability analysis based on the Wiener process integrated with historical degradation data. Qual Reliab Eng Int. 2023;39(4):1376–95. doi:10.1002/qre.3300.
4. Zhang Z, Si X, Hu C, Lei Y. Degradation data analysis and remaining useful life estimation: a review on Wiener-process-based methods. Eur J Oper Res. 2018;271(3):775–96. doi:10.1016/j.ejor.2018.02.033.
5. Wu D, Jia M, Cao Y, Ding P, Zhao X. Remaining useful life estimation based on a nonlinear Wiener process model with CSN random effects. Measurement. 2022;205(8):112232. doi:10.1016/j.measurement.2022.112232.
6. Hu Y, Zhu M, Lin H. A nonlinear Wiener process degradation model with damage resistance for reliability analysis. Ann Oper Res. 2025;352(1):169–92. doi:10.1007/s10479-025-06695-5.
7. Wang Y, Kang R, Chen Y. Belief reliability modeling for the two-phase degradation system with a change point under small sample conditions. Comput Ind Eng. 2022;173(14):108697. doi:10.1016/j.cie.2022.108697.
8. Zeng W, Tian X, Chen H, Sun W. Sealing degradation modeling and reliability analysis method of deep-water pipeline connector based on the two-phase nonlinear Wiener process. Model Simul Eng. 2024;2024(1):5427464. doi:10.1155/2024/5427464.
9. Ma J, Cai L, Liao G, Yin H, Si X, Zhang P. A multi-phase Wiener process-based degradation model with imperfect maintenance activities. Reliab Eng Syst Saf. 2023;232(8):109075. doi:10.1016/j.ress.2022.109075.
10. Guan Q, Wei X, Bai W, Jia L. Two-stage degradation modeling for remaining useful life prediction based on the Wiener process with measurement errors. Qual Reliab Eng Int. 2022;38(7):3485–512. doi:10.1002/qre.3147.
11. Zheng B, Chen C, Zhang W, Fu R, Hu Y, Lin Y, et al. Reliability estimation of complex systems based on a Wiener process with random effects and D-vine copulas. Microelectron Reliab. 2022;138(3):114640. doi:10.1016/j.microrel.2022.114640.
12. Yang Y, Suo B, Yin R, He Y. New fusion methods using a weighted L1 conflict measure for reliability assessment with multi-credibility evidence. Inf Sci. 2026;740(1):123173. doi:10.1016/j.ins.2026.123173.
13. Xu A, Wang B, Zhu D, Pang J, Lian X. Bayesian reliability assessment of permanent magnet brake under small sample size. IEEE Trans Rel. 2025;74(1):2107–17. doi:10.1109/TR.2024.3381072.
14. Zhang X, Chen W, Wang H, Li Y, Zhao Z, Wang W, et al. A novel multi-stage precision reliability assessment method for mechanical system by Bayesian fusion. Comput Ind Eng. 2025;200(12):110744. doi:10.1016/j.cie.2024.110744.
15. Zhang Q, Zhang P, Li T. Information fusion for large-scale multi-source data based on the Dempster-Shafer evidence theory. Inf Fusion. 2025;115(17):102754. doi:10.1016/j.inffus.2024.102754.
16. Yang C, Xiao F. An exponential negation of complex basic belief assignment in complex evidence theory. Inf Sci. 2023;622(4):1228–51. doi:10.1016/j.ins.2022.11.160.
17. Hua Z, Fei L, Xue H. Consensus reaching with dynamic expert credibility under Dempster-Shafer theory. Inf Sci. 2022;610(1):847–67. doi:10.1016/j.ins.2022.08.046.
18. Smets P. The combination of evidence in the transferable belief model. IEEE Trans Pattern Anal Machine Intell. 1990;12(5):447–58. doi:10.1109/34.55104.
19. Jahn KU. Evaluation of Hausdorff distances in interval mathematics. Computing. 1990;45(1):69–77. doi:10.1007/BF02250585.
20. You C, Yan L. The p-distance of uncertain variables. J Intell Fuzzy Syst. 2017;32(1):999–1006. doi:10.3233/JIFS-16959.
21. Bao YE, Peng XQ, Zhao B. The interval number distance and completeness based on the expectation and width. Fuzzy Syst Math. 2013;27(6):133–9. (In Chinese). doi:10.3969/j.issn.1001-7402.2013.06.021.
22. Ding J, Qiu J. An approach to improve the indicator weights of scientific and technological competitiveness evaluation of Chinese universities. Scientometrics. 2011;86(2):285–97. doi:10.1007/s11192-010-0268-7.

23. Sun Y, Li Y, Gu C, Zhang Q, Chen K. Dynamic reliability modeling and analysis of small modulus gear wear based on the Wiener process. Sci Rep. 2025;15(1):24537. doi:10.1038/s41598-025-09419-8.
24. Li S, Yan Z, Jia J. Reliability modeling method for constant stress accelerated degradation based on the generalized Wiener process. Entropy. 2025;27(12):1197. doi:10.3390/e27121197.
25. Liu D, Wang S. Reliability estimation from lifetime testing data and degradation testing data with measurement error based on evidential variable and Wiener process. Reliab Eng Syst Saf. 2021;205(1):107231. doi:10.1016/j.ress.2020.107231.
26. Ferson S, Oberkampf WL, Ginzburg L. Model validation and predictive capability for the thermal challenge problem. Comput Methods Appl Mech Eng. 2008;197(29–32):2408–30. doi:10.1016/j.cma.2007.07.030.
27. Ferson S, Oberkampf WL. Validation of imprecise probability models. Int J Reliab Saf. 2009;3(1–3):3. doi:10.1504/IJRS.2009.026832.